Journal of Alloys and Compounds 495 (2010) 33–38

Contents lists available at ScienceDirect

Journal of Alloys and Compounds

journal homepage: www.elsevier.com/locate/jallcom

Characterization of nanocrystalline CoCrFeNiTiAl high-entropy solid solution processed by mechanical alloying

K.B. Zhang[a], Z.Y. Fu[a,*], J.Y. Zhang[a], W.M. Wang[a], S.W. Lee[b], K. Niihara[c]

[a] State Key Laboratory of Advanced Technology for Materials Synthesis and Processing, Wuhan University of Technology, Wuhan 430070, China
[b] Department of Materials Engineering, SunMoon University, Asan, ChungNam 336-708, South Korea
[c] Extreme Energy-Density Research Institute, Nagaoka University of Technology, 1603-1 Nagaoka, Niigata 940-2188, Japan

ARTICLE INFO

Article history:
Received 31 August 2009
Received in revised form 3 December 2009
Accepted 3 December 2009
Available online 11 December 2009

Keywords:
Mechanical alloying
Microstructure
Thermal analysis
Consolidation

ABSTRACT

The equiatomic multicomponent CoCrFeNiTiAl high-entropy solid solution alloy was synthesized by mechanical alloying (MA). The effects of milling duration and subsequent annealing on the structure and morphology evolution were investigated. Supersaturated BCC and FCC solid solutions appear when the blended powder is ball milled more than 18 h. The 30 h ball milled alloy powder shows excellent chemical homogeneity and refined morphology with mean particle size of less than 5 μm. The microscaled particles are actually hard agglomerations of nanoscaled crystallines with crystal size of about 40 nm. The phase composition transforms to two BCC solid solutions when the 30 h mechanically alloyed powder was annealed at 600 °C for 1 h. The simple solid solution structure can be maintained even after the alloy was annealed at 1000 °C. The 30 h milled alloy powder was subsequently consolidated by spark plasma sintering (SPS) at 800 °C for 10 min. The sintered sample Exhibits 98% in relative density and 432 HV in Vickers hardness.

1. Introduction

Conventional concepts for alloy design are based on one principal element or compound to serve as a matrix for primary properties, with other minor elements incorporated for definite microstructure and properties, such as steels, TiAl intermetallics, bulk metallic glasses (BMG), etc. [1]. The main reason for not incorporating multi-principal elements into alloy preparation is the anticipated formation of many intermetallic compounds and other complex structures, resulting in sample brittleness, difficulty in processing and complication in analysis [2,3]. Recently, this paradigm has been broken by high-entropy alloy developed by Yeh et al. [4]. High-entropy alloys are defined as alloys that contain at least five principal elements with each elemental concentration between 5 and 35 at.%. The core principle behind the high-entropy alloy is the utilization of high configurational entropy in the liquid state or regular solid solution state, which leads to the formation of simple FCC and/or BCC solid solutions, nanosized precipitates and even amorphous phases [5–10]. The particular structures and properties offer many potential applications for high-entropy alloys, such as tools, moulds and mechanical parts, etc. [11,12].

Many high-entropy alloy systems have been exploited recently, and almost all of the blocky alloys were prepared by arc melt casting. However, the arc melt casting method can only prepare samples with limited shapes and sizes, which will definitely limit its industrial applications in the future. Mechanical alloying (MA) is a widely used solid state processing route for synthesis of advanced materials, which can easily lead to the formation of nanocrystalline and will definitely increase the properties and application scope of high-entropy alloys [13–16]. The CoCrFeNiTiAl$_x$ high-entropy alloy system had been investigated in our previous work and the results showed that the equiatomic CoCrFeNiTiAl alloy possessed excellent integrated mechanical properties [17]. In this paper, the CoCrFeNiTiAl high-entropy alloy powder was prepared by mechanical alloying and subsequent annealing to evaluate the structural evolution. The as-milled powder was consolidated by SPS and the structure and mechanical properties were investigated.

2. Experimental details

Co, Cr, Fe, Ni, Ti, Al elemental powders with purity of higher than 99.5% and particle size of ≤45 μm (325 mesh) were mechanically alloyed in equiatomic ratio. The milling was carried out up to 60 h in high energy planetary ball miller at 250 rpm with a ball to powder weight ratio of 15:1. High performance stainless steel vials and balls were utilized as the milling media and n-heptane was used as the process controlling agent (PCA). The powder samples were extracted at regular intervals of every 6 h. The 60 h

---

* Corresponding author. Tel.: +86 27 87865484; fax: +86 27 87215421.
E-mail address: zyfu@whut.edu.cn (Z.Y. Fu).

0925-8388/$ – see front matter © 2009 Elsevier B.V. All rights reserved.
doi:10.1016/j.jallcom.2009.12.010

milled powder was heat treated at different temperatures under flowing argon atmosphere. The 30 h ball milled alloy powder was subsequently sintered by SPS at 800 °C for 10 min in high purity argon atmosphere. The structure of alloys processed by different techniques was characterized by Rigaku Ultima III X-ray diffractometer (XRD) with Cu Kα radiation. The microstructure of the alloy powders was observed using scanning electron microscopy (SEM, Hitachi-S3400N) and high resolution transmission electron microscopy (HRTEM, JEOL Model-2100F). The chemical compositions of the milled powders were calculated from the results of energy-dispersive X-ray spectrometer (EDX) equipped with the SEM. The 30 h mechanically alloyed powder was embedded in an epoxy resin and then sliced by an ultramicrotome to facilitate the observation of transmission electron microscopy (TEM, JEOL JEM-2010). The thermal analysis was carried out in a NETZSCH STA 449C differential scanning calorimeter (DSC) at a heating rate of 5 K/min under flowing purified argon atmosphere. The relative density of the sintered sample was measured by the Archimedes method. Hardness measurements were conducted using a Vickers hardness tester (Wolpert-430SVD) under a load of 49 N for 15 s. At least seven tests were conducted to obtain the average value.

3. Results and discussions

3.1. X-ray analysis

Fig. 1 shows the XRD patterns of the equiatomic CoCrFeNiTiAl high-entropy alloy powders prepared under different milling durations. The primitive blending powder includes diffraction patterns of all alloy elements. The peak intensity decreases dramatically after the powder was grinded for 6 h. Obvious peak broadening can be observed and some peaks become invisible as the alloy powder was milled for 18 h. The intensity decrement and peak broadening are resulted from three points: refined crystal size, high lattice strain and decreased crystallinity [18]. However, the cause of diffraction peak disappearance is complicated, which can be introduced by: (1) particle and crystal refinement along with high lattice strain, (2) different atomic diffraction factor proportional to the atomic number, (3) crystallinity decrement (4) formation of solid solutions. As the milling time reaches up to 60 h, only the most intensive peaks (5 peaks) can be observed. The remnant peaks include the most intensive peaks of almost all alloys, which can eliminate the doubtful causes of fore-mentioned (2) and (3) of diffraction peak disappearance. Thus we can deduce the formation of solid solutions from the XRD patterns with milling duration more than 18 h and the peak disappearance is due to the crystal refinement, lattice distortion and solid solution.

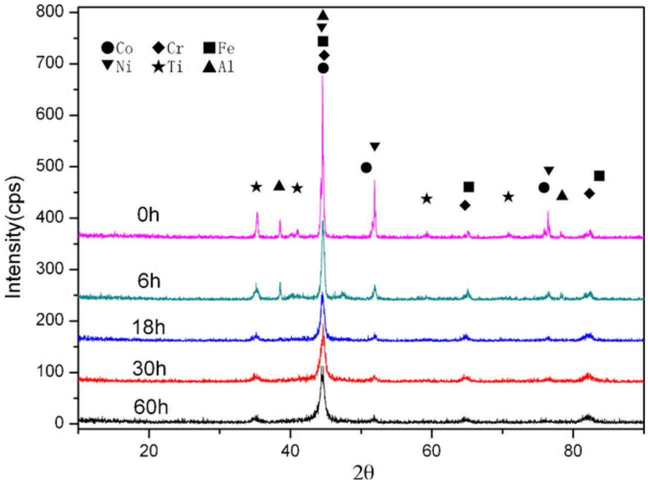

Fig. 1. XRD patterns of CoCrFeNiTiAl high-entropy alloy powders under different milling durations.

Table 1
The crystalline size (CS) and lattice strain of the CoCrFeNiTiAl high-entropy alloy powders under different milling times.

Milling time (h)	CoCrFeNiTiAl	
	CS (nm)	Lattice strain (%)
6	26	0.35
12	19	0.48
18	16	0.58
24	17	0.53
30	12	0.74
60	12	0.75

The crystal size and lattice strain of the alloy powders under different milling times have been calculated from the X-ray peak broadening using Scherrer' s formula after eliminating the instrumental contribution [14] (shown in Table 1). The crystal size is greatly refined as the milling duration increases. The 30 h mechanically alloyed powder exhibits a crystal size of 12 nm. The crystal size remains the same as that of 30 h when the powder was milled for 60 h. This means the equilibrium of crystalline refinement and cold welding is achieved when the alloy powder is milled for 30 h. The crystal size cannot be further refined with increased milling duration [23]. The lattice strain of the CoCrFeNiTiAl alloy powders increase as the milling prolongs. The 60 h milled alloy powder shows a lattice strain of 0.75%. Generally, the increment in lattice strain is due to: (1) the size mismatch effect between the constituents, (2) increasing grain boundary fraction and (3) mechanical deformation [19]. As the milling time increasing, the grain boundary fraction and mechanical deformation are continuously increased due to the decreased grain size. The increase in lattice strain may also result from the increased dislocation density produced by severe plastic deformation [20].

Table 2 shows the mixing enthopies of the metallic atomic pairs in the CoCrFeNiTiAl high-entropy alloy. Most of the atomic pairs exhibit high negative entropy. As we know that only atomic pair with mixing entropy near zero can possess high solid solubility [21]. On the other word, the CoCrFeNiTiAl high-entropy alloy possess limited solid solubility under equilibrium condition. However, the mechanically alloyed powder with milling duration more than 18 h shows simple solid solution structure. This kind of structure can be designated as supersaturated solid solution. The solid solubility extension is introduced by: (1) the effect of high mixing entropy and (2) the non-equilibrium state of the MA process. As the component element increases, radom diffusion between different elements is enhanced because of its high mixing entropy, which will definitely lead to the extension of solid solubility. In addition, the high entropy of mixing lowers the tendency to order and segregate, and makes the solid solution more easily formed and more stable than intermetallics and other ordered phases [5]. The MA process can extend the solid solubility limit as well. Alloying occurs as the grain size is refined down to nanometer range and thus a substantial amount of enthalpy can be stored in nanocrystal alloys due to the large grain boundary area. The energy stored in the grain boundaries serves as the driving force for the formation of solid solution [19,22]. The solid solubility is expected to extend among the multiple components with milling time increasing until it reaches a supersaturated level, after which no further extension of solid solubility will be achieved [6].

Table 2
The chemical mixing enthalpy(ΔH^{chem}) of binary equiatomic alloys calculated by Miedema's approach [17,24].

Element (atomic size, Å)	Co (1.25)	Cr (1.25)	Fe (1.24)	Ni (1.24)	Ti (1.44)	Al (1.43)
Co	–	−7	−1	0	−42	−19
Cr			−1	−7	−11	−10
Fe				−2	−25	−11
Ni					−52	−22
Ti						−30

3.2. Microstructure and chemical composition characterization

Fig. 2 depicts the SEM images of the CoCrFeNiTiAl high-entropy alloy powders under different milling times. The primitive powder exhibits a granular size of less than 50 μm. The particles firstly cold weld together to form even larger particles in the early period of mechanical alloying (as shown in Fig. 2(b) with 6 h of ball milling). The cold welded agglomerations are crushed down to smaller particles when the milling is prolonged. This circulation leads the powder be refined gradually and facilitates the diffusion and alloying among different metallic elements. An equilibrium between the crushment and fragmentation is achieved at a certain milling duration (30 h in this research). The 30 h mechanically alloyed powder reveals an average particle size of less than 5 μm as shown in

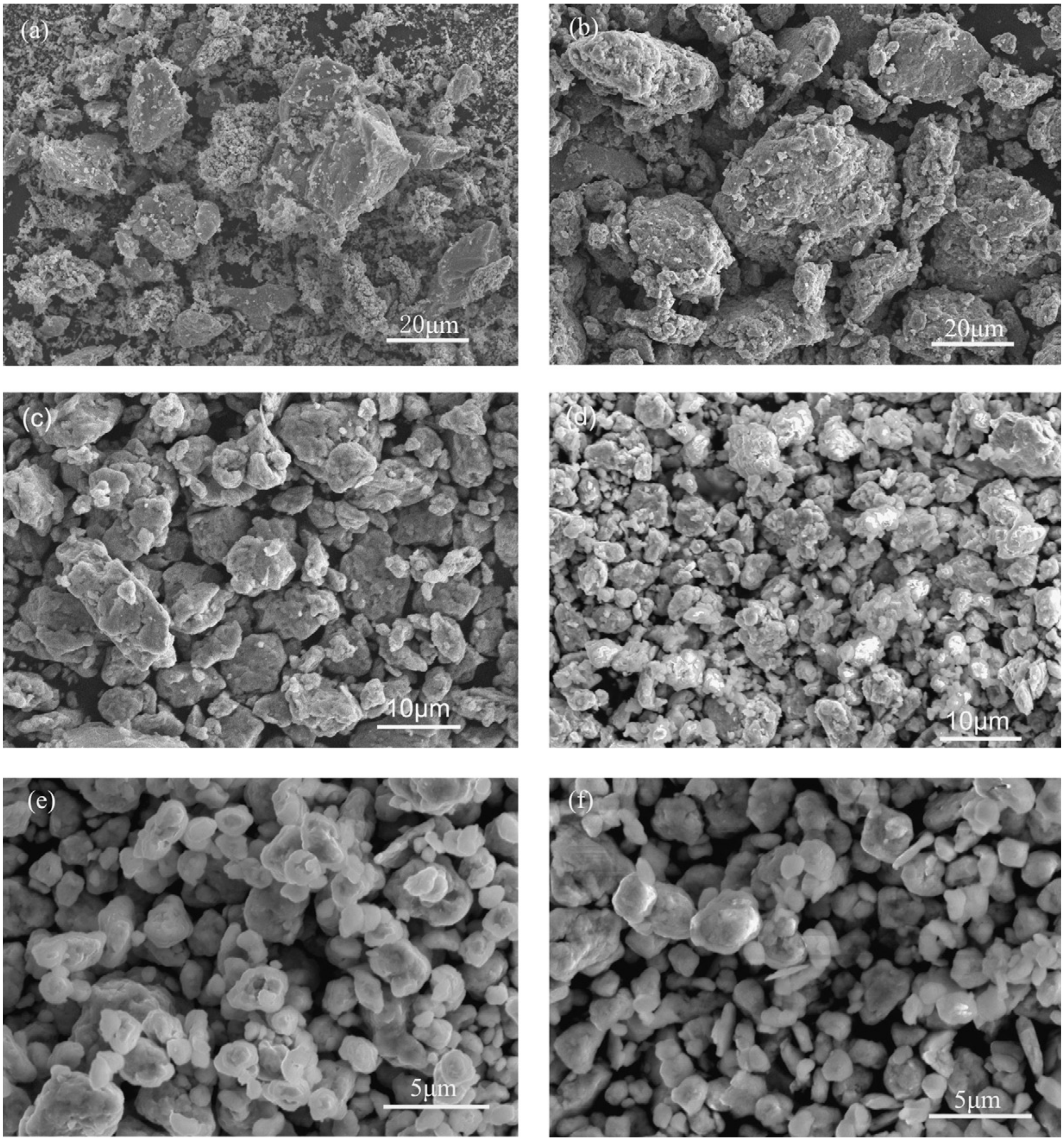

Fig. 2. SEM images of CoCrFeNiTiAl high-entropy alloy powders under different milling durations: (a) 0 h, (b) 6 h, (c) 18 h, (d) 30 h, (e) 60 h, (f) 60 h + 2 h wet milled.

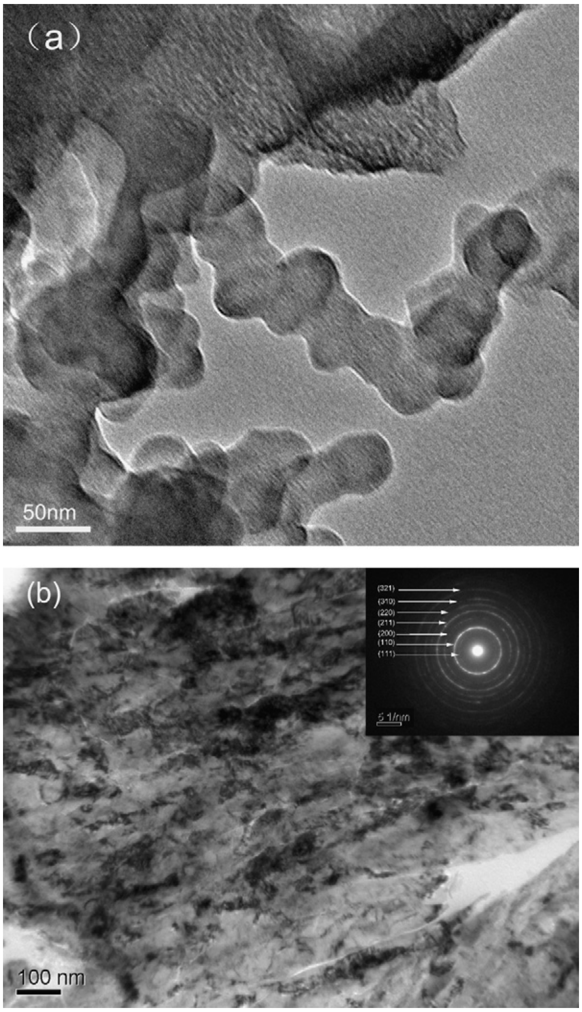

Fig. 3. TEM images of the 60 h MA CoCrFeNiTiAl high-entropy solid solution: (a) HRTEM image, (b) TEM bright field image and corresponding SAED pattern.

Fig. 2(d). Further refinement has not taken place when the milling time reaches 60 h (Fig. 2(e)). Different from the 30 h milled powder, the 60 h milled powder shows a more smooth morphology and spherical shaped particle. The 60 h milled alloy powder is subsequently wet ball milled 2 h with alcohol as the milling media. Some of the elliptical shaped particles are scraped to a lamellar structure with thickness of less than 1 μm (shown in Fig. 2(f)). This phenomenon indicates that the mechanically alloyed microscaled alloy powder is actually hard agglomerated particles of nanoscaled crystallines. The nanoscaled crystals form thin sheets and then they file up to form relatively larger elliptical shaped particles. The EDX microanalysis results (not listed in this paper) exhibit the excellent chemical homogeneity and the equiatomic composition of alloy particles after 30 h of ball milling.The nanostructure of the 30 h ball milled CoCrFeNiTiAl high-entropy alloy powder is confirmed by the HRTEM image shown in Fig. 3(a). The particle shows an agglomerated morphology of nanoscaled crystallines with crystal size of about 40 nm. The observed crystal size is much larger than that calculated by the Scherrer's formula. This discrepancy may be introduced by the calculating methodology when using the FWHM to estimate the crystal size refinement. The nanoscaled crystal can also be seen in the TEM bright field image in Fig. 3(b). The simple solid solution structure is further confirmed by the selected area electron diffraction (SAED) shown in Fig. 3(b). The ring pattern reveals the polycrystalline structure of the 30 h alloyed powder with a strong ordered BCC structure and a weak disordered FCC phase. The SAED pattern indicates that the BCC solid solution is the main phase while the FCC solid solution as the minor phase.

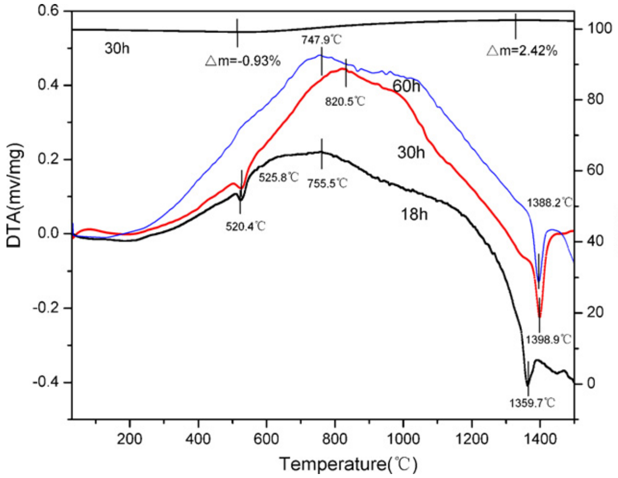

Fig. 4. DSC curves of CoCrFeNiTiAl high-entropy alloy powder ball milled 18, 30 and 60 h, and the TG curve of the 30 h milled alloy.

3.3. Thermal analysis, annealing treatment and powder consolidation

Fig. 4 depicts the DSC curves of the mechanically alloyed CoCrFeNiTiAl high-entropy powders under different milling durations. The 18 h, 30 h and 60 h mechanically alloyed powders exhibit analogous exothermic/endothermic trends in the temperature range of 25–1500 °C. However, the alloy with longer milling time shows higher exothermic energy in the whole range. The long exothermic line from 25 to 525 °C is associated with the release of internal stresses, such as structural deformation, lattice strain, etc. The 18 h and 30 h ball milled powder reveal endothermic peaks at 520.4 and 525.8 °C, respectively. This energy absorption can be related to the phase transformation to form another BCC phase, which will be illustrated in the next part. The exothermic peaks over 600 °C (at approximately 755.5, 820.5.0 and 747.9 °C) are related to the energy release of phase transformation. The 60 h milled alloy powder exhibits no endothermic peak of PCA evaporation because of its higher exothermic effect during the phase transformation, which counteract the energy absorption of the PCA evaporation. The exothermic energy increases as the alloy was ball milled with longer duration, which is because of the increment in lattice strain, grain boundary and refined grain size. The exothermic energy of the 18, 30 and 60 h ball milled alloys are estimated to be 0.22, 0.44 and 0.48 mV/mg, respectively. Long endothermic curves appear after the exothermic peaks and it can be associated with gradual collapse of the crystalline structure under high temperature. The endothermic peaks appear at 1359.7, 1398.9 and 1388.2 °C are designated as the alloys' melting points. The TG curve inserted in Fig. 4 indicates the weight change of the 30 h mechanically alloyed powder. The gross weight decreases firstly and then increases as the temperature rising. 2.42% of total weight grain is achieved when the temperature reaches the melting point. The weight lose is result from the evaporating of PCA and other phases with low melting points while the weight gain can be attributed to the surface oxidation.

The 30 h mechanically alloyed CoCrFeNiTiAl high-entropy alloy powder was annealed 1 h at different temperatures and their XRD patterns are listed in Fig. 5(a). The powder shows thermal stability up to 500 °C. Phase transformation begins at 520 °C. So we can see diffraction peaks corresponding to two BCC solid solutions obviously in the 600 °C annealed alloy. An FCC phase precipitates

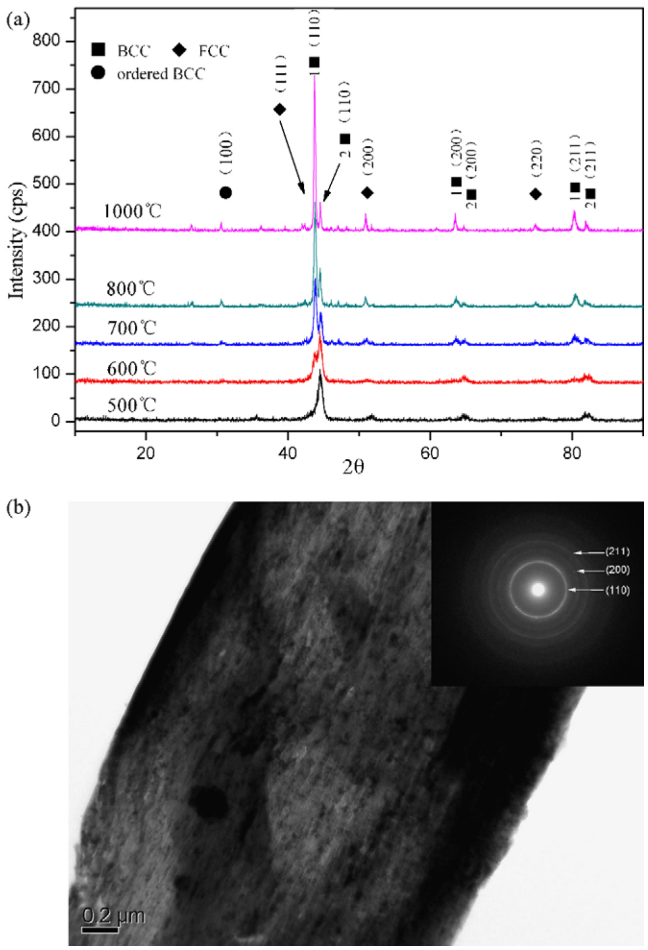

Fig. 5. (a) XRD patterns of the 30 h ball milled CoCrFeNiTiAl high-entropy solid solution under different annealing temperatures, (b) TEM bright field image and corresponding SAED pattern of the 700 °C annealed sample.

as a minor phase when the alloy was annealed at 700 °C for 1 h. The 700 °C annealed alloy powder shows identical crystal structure as the as-cast CoCrFeNiTiAl high-entropy alloy prepared by arc melt casting [15]. The alloy is also composed of simple solid solution phases after been annealed at 800 °C, but the diffraction peak intensity increases significantly. No obvious change can be observed in the 1000 °C annealed alloy. The solid solution structure is maintained with its peak intensity increased further. The increment of diffraction intensity is resulted from the crystal coarsening and internal energy release during the annealing process. The phase transformation under different annealing temperatures is attributed to the metastable state of the supersaturated solid solutions. This metastable structure transforms to stable equilibrium ones in the final stage of annealing [20]. Fig. 5(b) shows the TEM bright field image and the corresponding SAED of the 30 h ball milled after be annealed at 700 °C for 1 h. The nanosized structure is observed and simple BCC solid solution structure is further confirmed.

To facilitate its industrial applications, the mechanically alloyed CoCrFeNiTiAl high-entropy alloy powder should be consolidated to form dense blocky samples with desired shapes and properties. In this paper, a novel technology of spark plasma sintering (SPS) was exploited for the densification of the 30 h ball milled alloy powder. The SPS was conducted at 800 °C for 10 min in an argon atmosphere with a sintering pressure of 30 MPa. The XRD patterns (shown in Fig. 6) reveal that the sintered bulky sample is consisted of simple solid solution structure, which is the same as that of the 800 °C annealed alloy powder. The relative density and Vickers hardness were measured for the densified alloy. 98% of relative density and 432 HV of Vickers hardness are achieved after the powder was sintered by SPS at 800 °C. The consolidation results suggest that the mechanically alloyed CoCrFeNiTiAl high-entropy alloy can be quickly densified with high strength, which will definitely broaden the industrial application of high-entropy alloys.

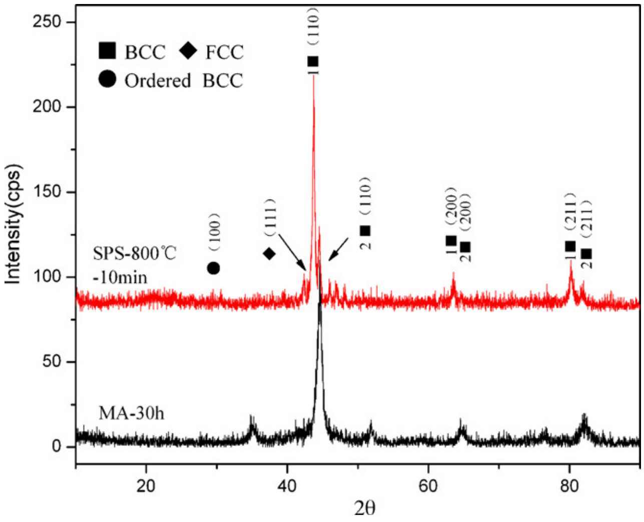

Fig. 6. XRD pattern of the 30 h milled sample sintered at 800 °C by SPS.

4. Conclusions

The equiatomic CoCrFeNiTiAl high-entropy alloy has been successfully synthesized by mechanical alloying. Supersaturated solid solutions can be obtained when the blended powder is milled more than 18 h. The 30 h ball milled alloy powder shows a mean particle size of less than 5 μm, which is actually hard agglomeration of nanosized crystallines with crystal size of about 40 nm. The 60 h mechanically alloyed powder contains high lattice strain of 0.75% and exhibits excellent chemical homogeneity. The structure transforms to two BCC phases when it is annealed at 600 °C for 1 h. Another minor FCC phase precipitates after be annealed at 700 °C. The phase transformation under different annealing temperatures is attributed to the formation of metastable supersaturated solid solution during the mechanical alloying process. The 30 h mechanically alloyed CoCrFeNiTiAl powder can be quickly densified by SPS. The 800 °C sintered solid solution sample shows a relative density of 98% and high Vickers hardness of 432 HV, indicating good sinterability and high strength of the mechanically alloyed CoCrFeNiTiAl high-entropy alloy.

Acknowledgements

The authors would like to acknowledge the financial support by the National Natural Science Foundation of China under granted no. 50772081 and no. 50821140308, and the Ministry of Education of China under granted no. PCSIRT0644.

References

[1] A. Inoue, Acta Mater. 48 (2000) 1383–1395.
[2] A.L. Greer, Nature 383 (1996) 150.
[3] H. Baker, Metals Handbook, vol. 3, 10th ed., ASM International, Metal Park, OH, 1992.
[4] J.W. Yeh, S.K. Chen, S.J. Lin, J.Y. Gan, T.S. Chin, T.T. Shun, C.H. Tsau, S.Y. Chang, Adv. Eng. Mater. 6 (2004) 299–303.
[5] J.W. Yeh, Ann. Chim. Sci. Mater. 31 (2006) 633–648.

[6] C.J. Tong, Y.L. Chen, S.K. Chen, J.W. Yeh, T.T. Shun, C.H. Tsau, S.J. Lin, S.Y. Chang, Metall. Mater. Trans. A 36A (2005) 881–893.
[7] Y.J. Zhou, Y. Zhang, Y.L. Wang, G.L. Chen, Appl. Phys. Lett. 90 (2007) 181904.
[8] B. Cantor, I.T.H. Chang, P. Knight, A.J.B. Vincent, Mater. Sci. Eng. A 375 (2004) 213–218.
[9] Y.J. Zhou, Y. Zhang, Y.L. Wang, G.L. Chen, Mater. Chen. Sci. Eng. A 454 (2007) 260.
[10] Y.P. Wang, B.S. Li, M.X. Ren, C. Yang, H.Z. Fu, Mater. Sci. Eng. A 491 (2008) 154–158.
[11] C.P. Lee, C.C. Chang, Y.Y. Chen, J.W. Yeh, H.C. Shih, Corros. Sci. 50 (2008) 2053–2060.
[12] Y. Zhang, Y.J. Zhou, P.L. Jin, G.L. Chen, K.L. Peter, Adv. Eng. Mater. 6 (2008) 534–538.
[13] C. Suryanarayana, Prog. Mater. Sci. 46 (2001) 45–62.
[14] S. Varalakshmi, M. Kamaraj, B.S. Murty, J. Alloys Compd. 460 (2008) 253–257.
[15] K.B. Zhang, Z.Y. Fu, J.Y. Zhang, W.M. Wang, H. Wang, Y.C. Wang, Q.J. Zhang, J. Shi, J. Alloys Compd. 485 (2009) L31–L34.
[16] Y.L. Chen, Y.H. Hu, C.W. Tsai, C.A. Hsieh, S.W. Kao, J.W. Yeh, T.S. Chin, S.K. Chen, J. Alloys Compd. 477 (2009) 696–705.
[17] K.B. Zhang, Z.Y. Fu, J.Y. Zhang, W.M. Wang, H. Wang, Y.C. Wang, Q.J. Zhang, J. Shi, Mater. Sci. Eng. A 508 (2009) 214–219.
[18] J.W. Yeh, S.Y. Chang, Y.D. Hong, S.K. Chen, S.J. Lin, Mater. Chem. Phys. 103 (2007) 41–46.
[19] H.X. Sui, M. Zhu, M. Qi, G.B. Li, D.Z. Yang, J. Appl. Phys. 71 (1993) 2945–2949.
[20] A.R. Yavari, P.J. Desre, T. Benameur, Phys. Rev. Lett. 68 (1992) 2235–2238.
[21] A. Takeuchi, A. Inoue, Mater. Sci. Eng. A 304 (2001) 446–451.
[22] B.L. Huang, R.J. Perez, E.J. Lavernia, M.J. Luton, NanoStructured Mater. 7 (1996) 67–69.
[23] L. Schultz, Philos. Mag. B 61 (1990) 453–471.
[24] H. Zhang, B.W. Zhang, L.J. Wu, Z.Q. Wan, Acta Phys. Sin. 43 (1994) 1638.